ELSEVIER

Journal of Alloys and Compounds 452 (2008) 48–53

Journal of ALLOYS AND COMPOUNDS

www.elsevier.com/locate/jallcom

Solidus and liquidus of plutonium and uranium mixed oxide

Masato Kato [a,*], Kyoichi Morimoto [a], Hiromasa Sugata [b], Kenji Konashi [c], Motoaki Kashimura [a], Tomoyuki Abe [a]

[a] *Japan Atomic Energy Agency, 4-33 Muramatsu, Tokai-mura, Naka-gun, Ibaraki 319-1194, Japan*
[b] *Inspection Development Company, 4-33 Muramatsu, Tokai-mura, Naka-gun, Ibaraki 319-1194, Japan*
[c] *Tohoku University, 2145-2 Narita-chou, Oarai-chou, Ibaraki 311-1313, Japan*

Received 18 September 2006; received in revised form 18 January 2007; accepted 19 January 2007
Available online 12 March 2007

Abstract

Solidus and liquidus of mixed oxides of plutonium and uranium were measured as a function of Pu-content and oxygen-to-metal ratio using the thermal arrest technique. The solidus and the liquidus were observed to decrease with increasing Pu-content and to slightly increase with decreasing oxygen-to-metal ratio in the region of hypo-stoichiometric composition. The solidus of $UO_{2.00}$, $(Pu_{0.12}U_{0.88})O_{2.00}$ and $(Pu_{0.2}U_{0.8})O_{2.00}$ were determined as 3128, 3077 and 3052 K, respectively. The solidus and the liquidus of the mixed oxides with 29 and 40 at% Pu were also measured. It was observed that a reaction with the tungsten capsule occurred during the measurement. Therefore, the solidus and the liquidus of the oxides with 29 and 40 at% Pu could not be obtained.

Keywords: Phase diagrams; Thermal analysis; Actinide alloys and compounds; Nuclear materials; Oxide materials

1. Introduction

The mixed oxides of plutonium and uranium (MOX) have been developed as a fuel for fast reactors. The maximum temperature of the fuel pellets during irradiation is limited to prevent fuel melting. So, the solidus and the liquidus of the mixed oxides have been investigated ever since the development of fast reactors was started [1–11]. However, the measured data are still limited because of difficulties in preparing MOX samples with precise oxygen-to-metal (O/M) ratios and in conducting accurate measurements at high temperature on plutonium containing samples.

Early studies [3–5] related to the melting process of oxide fuels were carried out using the V-filament technique. In this method the melting process was observed using a small sample on a heated tungsten ribbon in both hydrogen and helium atmosphere. However, it was reported that the data measured by the V-filament method had a large error caused by variation of the composition of the sample during measurements [6,7]. Consequently, the solidus and the liquidus can be derived in a more reliable manner from the thermal arrests observed by measuring the temperature during heating or cooling of samples encapsulated in tungsten capsules. Baichi et al. [12] fully explained the reason of the large error in the V-filament method and concluded that the samples have to be encapsulated. Lyon and Baily [6] and Aitken and Evans [8] measured the solidus and the liquidus of the mixed oxide systematically by the thermal arrest method. Lyon and Baily [6] reported the solidus and the liquidus of the UO_2–PuO_2 system, and Aitken and Evans [8] investigated the solidus and the liquidus of $(Pu, U)O_{2-x}$ as a function of the Pu-content and the O/M-ratio. However, both studies did not report results of analyses such as a microstructure and a lattice parameter of the samples after the measurements of the solidus and the liquidus.

In the present study the solidus and the liquidus of UO_2 and MOX containing Pu up to 40 mol% of PuO_2 were measured as a function of the Pu-content and the O/M-ratio using the thermal arrest technique. The trend of the solidus and the liquidus is discussed in the U-rich region of the Pu–U–O ternary system through analyses of samples before and after the measurements.

* Corresponding author. Tel.: +81 29 282 1111; fax: +81 29 282 9473.
E-mail address: kato.masato@jaea.go.jp (M. Kato).

0925-8388/$ – see front matter © 2007 Elsevier B.V. All rights reserved.
doi:10.1016/j.jallcom.2007.01.183

Table 1
Starting and ending points of the melting process obtained in mixed oxides

Sample	O/M-ratio	Temperature of melting (K)	
		Starting point (±35 K)	Ending point (±50 K)
$UO_{2.00}$	2.000	3140	3145
	2.000	3111	3130
	2.000	3134	3173
$(Pu_{0.12}U_{0.88})O_{2-x}$	2.000	3077	3117
	1.989	3093	3135
	1.983	3084	3105
	1.975	3085	3107
	1.974	3054	3069
	1.971	3100	3124
$(Pu_{0.2}U_{0.8})O_{2-x}$	2.000	3052	3090
	1.982	3059	3089
	1.967	3066	3079
	1.954	3074	3109
	1.950	3079	3097
	1.942	3092	3118
$(Pu_{0.29}U_{0.71})O_{2.00}$	2.000	2967	3047
$(Pu_{0.4}U_{0.6})O_{2.00}$	2.000	2910	3024

2. Experimental

2.1. Sample preparation

Sintered pellets of $UO_{2.00}$, $(Pu_{0.12}U_{0.88})O_{2-x}$, $(Pu_{0.2}U_{0.8})O_{2-x}$, $(Pu_{0.29}U_{0.71})O_{2-x}$ and $(Pu_{0.4}U_{0.6})O_{2-x}$ were prepared as samples for measuring solidus and liquidus. Three kinds of powder, $(Pu_{0.12}U_{0.88})O_{2+x}$, $(Pu_{0.2}U_{0.8})O_{2+x}$ and $(Pu_{0.29}U_{0.71})O_{2+x}$, were obtained by adjusting the Pu/U ratio in nitric acid solution and then treating the specimens by the micro-wave-heating denitration-method [13]. A mixed powder of composition of $(Pu_{0.4}U_{0.6})O_{2-x}$ was prepared from UO_2 and PuO_2 powders by ball milling. All of them were pressed and sintered at 1973 K for 5 h in an atmosphere of Ar and 5% H_2 gas mixture with added moisture. The sintered pellets were adjusted to an O/M-ratio of 2.00 by annealing at 1023 K for 5 h at the oxygen potential of $\Delta\bar{G}_{O_2} \cong -400$ kJ/mol. Then the pellets of $(Pu_{0.12}U_{0.88})O_{2.00}$ and $(Pu_{0.2}U_{0.8})O_{2.00}$ were annealed under appropriate conditions to obtain hypo-stoichiometric MOX pellets with a variety of O/M values [14–16]. Table 1 lists the composition of the pellets prepared in this study.

The impurities in the sample were analyzed by atomic emission spectrophotometry and γ-ray spectrometry. The sum of metallic impurities in the pellet was less than 500 ppm and the Am-contents contained in the $(Pu_{0.12}U_{0.88})O_{2-x}$, $(Pu_{0.2}U_{0.8})O_{2-x}$, $(Pu_{0.29}U_{0.71})O_{2-x}$ and $(Pu_{0.4}U_{0.6})O_{2-x}$ were 0.2, 0.4, 0.3 and 0.5 at% of the total metal amount, respectively.

2.2. Measurement procedures

The apparatus and procedures for determining the solidus and the liquidus of MOX used in this work were similar to those described previously [6–11]. Samples of about 10 g were taken from crushed pellets. The samples were loaded into tungsten capsules (40 mm long × 14 mm inner diameter) and were sealed in a vacuum of 2×10^{-2} Pa by electronic beam welding. The capsule and sample were heated at a constant heating rate of about 40 K/min to 3000 K or higher with a radiofrequency heating furnace. Details of the apparatus were reported previously [11]. After the measurement, the samples were removed from the capsules and were analyzed by ceramography, X-ray diffraction (XRD; Rigaku, RINT 1100) and electron probe micro analysis (EPMA; JEOL, JAX8800). The results were compared with the data measured before heating treatments.

Temperatures were observed with a pyrometer viewing the black body well which was fabricated into the bottom cap of the tungsten capsule. The temperature was calibrated by measuring the melting points of tantalum, molybdenum, niobium and alumina, which were reported to be 3280, 2895, 2745, and 2326 K, respectively [17]. The observed melting points of the standards were fitted by a linear correlation function, and the deviations from nominal temperature were corrected by the fitting curve. The true temperatures were obtained from the observed temperature using the calibration curve computed before or after the melting experiment. The maximum errors of solidus and liquidus were estimated to be ±35 and ±50 K respectively, since the error in the measurement of the standard was ±20 K and that introduced by the curve fitting was ±15 and ±30 K, respectively.

3. Results

Fig. 1 shows the temperature curves during the heating of $(Pu_{0.2}U_{0.8})O_{2-x}$. In these curves the changes in temperature due to thermal arrest were observed clearly (marked by arrows). The starting and ending points of thermal arrest are listed in Table 1. The temperature of the thermal arrest decreased gradually with increased Pu-content and O/M-ratio.

The samples were analyzed by X-ray diffraction. The lattice parameters determined before and after the measurements are shown in Fig. 2 together with the values from previous calculations [18]. Lattice parameters of UO_2, $(Pu_{0.12}U_{0.88})O_{2-x}$ and $(Pu_{0.2}U_{0.8})O_{2-x}$ both before and after heating were in good agreement with the calculated ones. The lattice parameters of the melted samples of $(Pu_{0.29}U_{0.71})O_{2.00}$ and $(Pu_{0.4}U_{0.6})O_{2.00}$ were larger than those obtained before heating. The differences may be explained by a variation of the Pu-content or the O/M-ratio which might have occurred during the measurement.

Fig. 3 shows the microstructure of the samples after the melting experiment. The metallic inclusions, which were observed in the microstructure of $(Pu_{0.29}U_{0.71})O_{2.00}$ and $(Pu_{0.4}U_{0.6})O_{2.00}$, were identified by X-ray diffraction and EPMA as metallic tungsten. It was confirmed that the amount of the metallic phase was less than 1 at% in samples with Pu content of 0–20 at% and more than 5 at% in samples with 29–40 at% Pu.

Fig. 4 shows the mapping images of U Lα, Pu Mα and W Kα from EPMA for a section of a $(Pu_{0.4}U_{0.6})O_{2.00}$ sample after the measurement. According to these images, the phases of plutonium oxide and tungsten were present in the melted sample. Such phases were also observed in the measurements of $(Pu_{0.3}U_{0.7})O_{2.00}$. Contrary to the observation, there is no

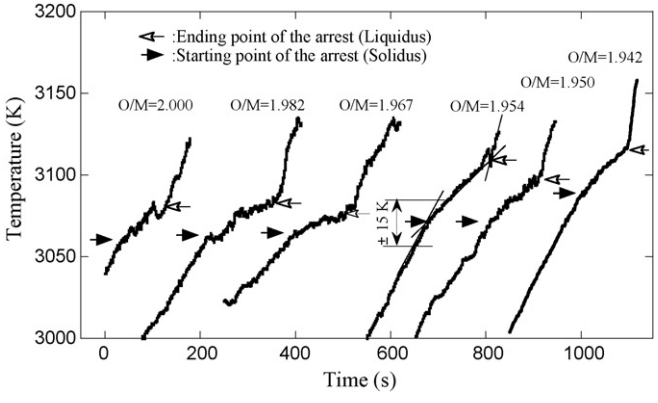

Fig. 1. Heating temperature curves measured on samples of $(Pu_{0.2}U_{0.8})O_{2-x}$ of different O/M-ratios.

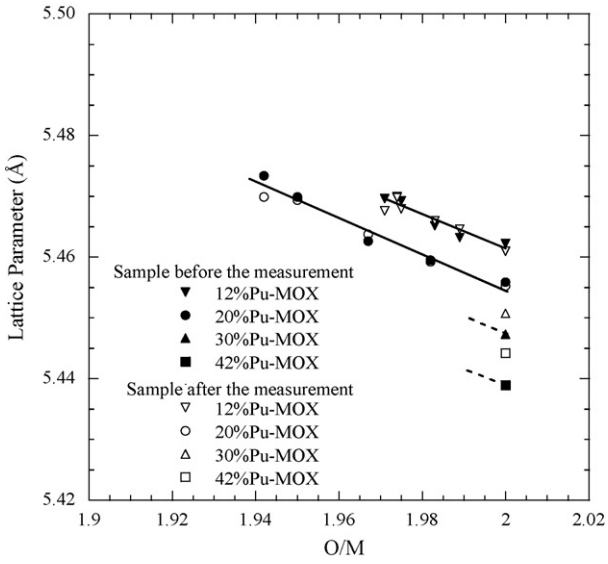

Fig. 2. Lattice parameters of mixed oxides before and after the melting experiment.

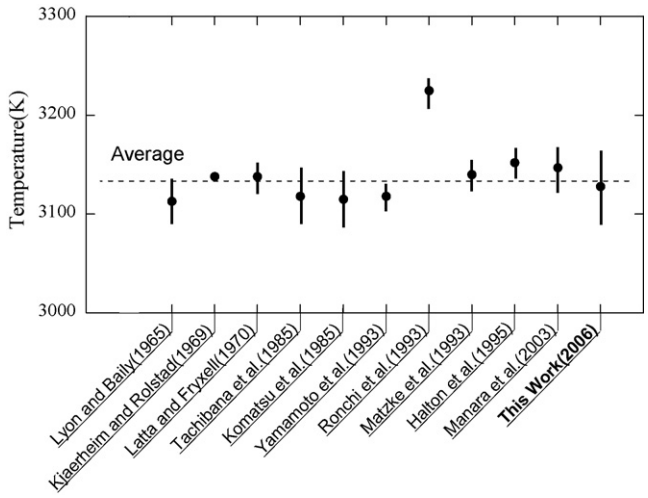

Fig. 5. Comparison of melting points of $UO_{2.00}$. The data were plotted in reported order.

precipitation of an independent Pu-oxide in the presently known phase diagram [6,8,19].

4. Discussion

Many studies on the melting point of UO_2 have been carried out previously. Lyon and Baily [6] reported the melting point was 3113 K, while Latta and Fryxell [7] measured the solidus and the liquidus of $UO_{2\pm x}$ and reported 3149 K for the melting point of $UO_{2.00}$. Recently Baichi et al. [12] reviewed the melting temperature of $UO_{2\pm x}$ and recommended a value of 3138 ± 15 K for $UO_{2.00}$. Fig. 5 compares the melting point of UO_2 observed in previous studies [6,7,9,12,20–26]. The melting point of $UO_{2.00}$ observed in the present work was 3128 ± 35 K which is in good agreement with the average of those earlier works. The error of the measurement in this work is lager than those of previous

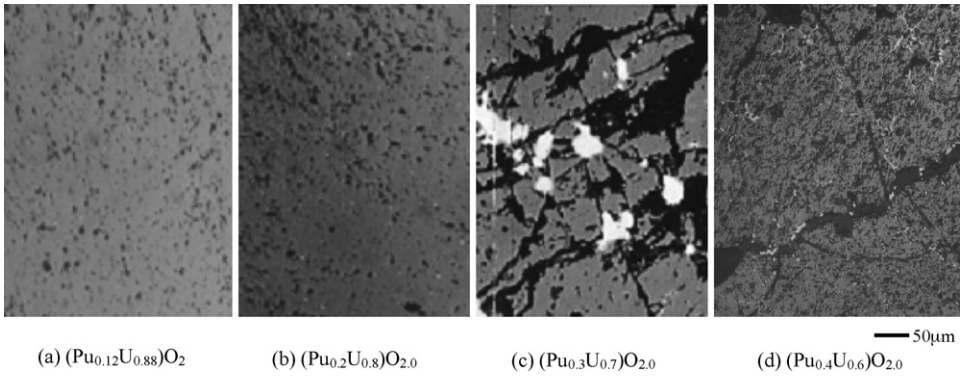

Fig. 3. Microstructures of samples after the melting. The white phase was identified as metallic W.

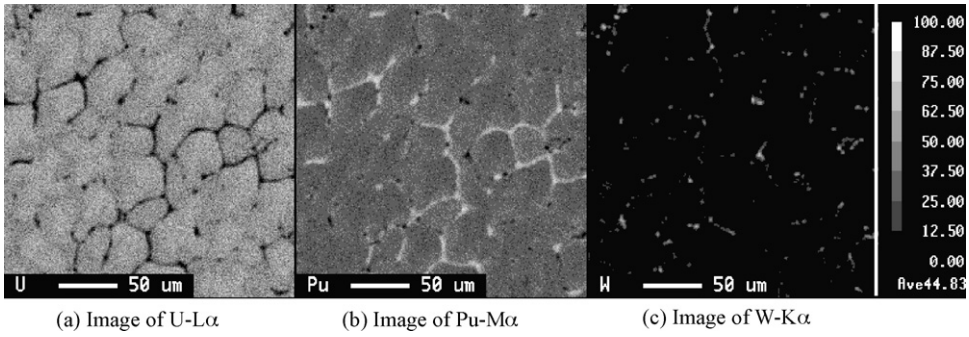

Fig. 4. Mapping images of $(Pu_{0.4}U_{0.6})O_{2.00}$ analyzed by EPMA. Distributions of U, Pu, and W were analyzed on the sample area of the melted sample.

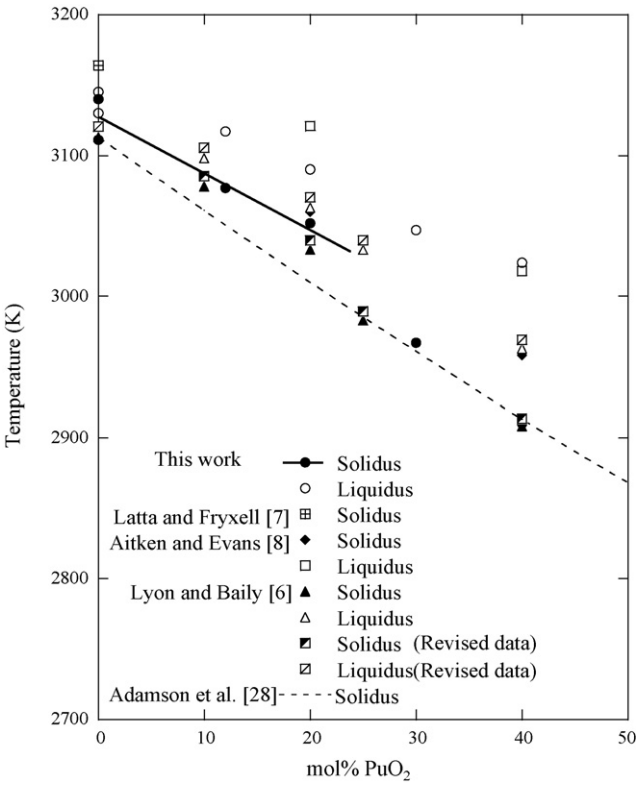

Fig. 6. Variation of the solidus and the liquidus in the UO_2–PuO_2 system with the sample composition.

works, most of them estimated from deviations caused by limited reproducibility of the melting points of the standards. In this work curve fitting error was taken into account in addition to the variation of standards (Fig. 2).

Fig. 6 shows the solidus and the liquidus of the UO_2–PuO_2 solid solution. The solidus and the liquidus reported by Lyon and Baily [6] are also plotted for comparison. They calibrated the temperature by using standard samples of Ta, Mo, Nb, Al_2O_3 and Pt, which have melting points of 3269, 2893, 2741, 2323 and 2046 K, respectively. However, their melting points were revised to 3280, 2895, 2745, 2326 and 2041 K, respectively [17]. These revised data were used for calibration in this work. Considering the changes in melting points of the standard samples, the solidus and the liquidus reported by Lyon and Baily [6] are found to be shifted to higher temperatures by 7–8 K as apparent in Fig. 6. The revised solidus is in good agreement with the present data.

The solidus and the liquidus in the system UO_2–PuO_2 were evaluated by an ideal solution model [27]. Recently, Carbajo et al. [1] reviewed thermodynamic data of MOX and recommended the equation for the solidus and the liquidus of the UO_2–PuO_2 system as reported by Adamson and Aitken [28]. The solidus reported by Adamson and Aitken [28,29] is shown by the broken line in Fig. 6. The calculation result is in good accordance with the solidus and the liquidus of MOX with Pu-content of more than 25 at%. On the other hand, the calculation underestimates the solidus of samples with Pu-contents of 12 and 20 at%. The solid line shown in Fig. 6 refers to the present data of samples with 0–20 mol% PuO_2. The solidus of MOX with 40 at% Pu is about 100 K lower than extrapolated solid line. It can be assumed that the reaction of samples with the tungsten capsule affects the measurement of the solidus and the liquidus of samples with high Pu-contents. This assumption was based on the following findings: the samples before and after the measurement were analyzed by XRD, ceramography and EPMA. The results of the analyses showed that the MOX with 29 and 40 at% Pu reacted with the tungsten capsule and a large amount of metallic tungsten mixed into the MOX during heating to the melting. The solidus of samples with Pu-content of more than 29 at% decreased significantly from the solidus of the MOX with 0–20 at% Pu-content. It was considered that the reaction between MOX and tungsten resulted in the decrease of solidus. It is well known that the oxygen potential of MOX increases with increasing Pu-content in the UO_2–PuO_2 system [14,15]. The increase of the oxygen potential might cause the reaction with tungsten in MOX with 29 and 40 at% of Pu. Additional examinations taking account of capsule materials are essential to explain the mechanism of the reaction with tungsten.

The Pu-oxide was observed along the grain boundaries in the melted samples with 29 and 40 at% of Pu, and the precipitation of the Pu-oxide caused the decrease of the Pu-content inside the grain. It was considered that the significant increase of the lattice parameters after the measurement shown in Fig. 4 was caused by the variation of Pu-content inside the grain. In fact, the lattice parameter of the melted sample with Pu-oxide and metallic tungsten was in agreement with the Pu-content inside the grain analyzed by EPMA.

Some studies [30–32] on the reaction between UO_2 and metallic elements have been reported. Fujino et al. [30] investigated the microstructure of UO_2 with the addition of 3.5 at% Ti and observed the eutectic phase of UO_2 and Ti-oxide on the grain boundary. Yamanaka et al. [31] also investigated the reaction of UO_2 and metallic Ti on the grain boundaries, and reported that the liquid phase appears at 1573 K which is lower than melting points of UO_2 and Ti. The reaction reported in the UO_2–Ti system is similar to the reaction observed in this work. It was assumed that thermal arrest observed in the measurements of $(Pu_{0.29}U_{0.71})O_{2.00}$ and $(Pu_{0.4}U_{0.6})O_{2.00}$ was not the melting of MOX. Investigating the equilibrium phase diagram in the Pu–W–O system might be important in the quantitative evaluation of the modification of the melting behaviour.

Fig. 7 plots the melting behaviour of $(Pu_{0.12}U_{0.88})O_{2-x}$ and $(Pu_{0.2}U_{0.8})O_{2-x}$ in variation with the O/M-ratio. Both solidus increased slightly with decreasing O/M-ratio. Aitken and Evans [8] measured the solidus and the liquidus as a function of Pu-content and O/M-ratio. Adamson and Aitken [28,29] revised down the values of the earlier their work [8] by re-calibrating the temperature using the measured melting point of UO_2 which is shown in Fig. 7(b). The slight difference between the data in this and other works would be caused by the difficulty in measuring the temperature in such a high temperature range.

The phase diagrams of U–O and Pu–O system are essential to evaluate the solidus and the liquidus in the hypo-stoichiometric composition of MOX. Many studies [12,33,34] on the phase diagram of the U–O system have been reported, and a ther-

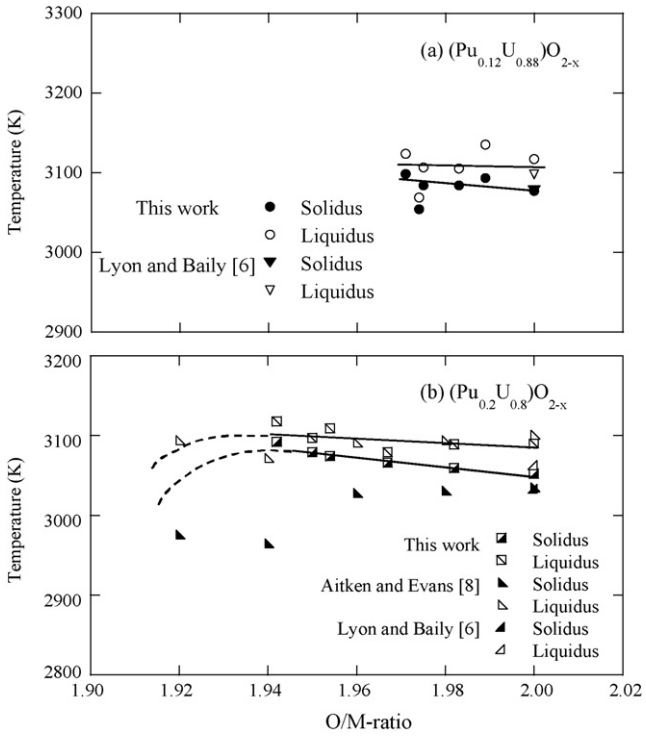

Fig. 7. Effect of the O/M-ratio on the solidus and the liquidus of (a) $(Pu_{0.12}U_{0.88})O_{2-x}$ and (b) $(Pu_{0.2}U_{0.8})O_{2-x}$.

modynamics database of the system has been constructed. It was reported that $UO_{2\pm x}$ has a congruent melting point at O/U-ratio of 2.00 and that the solidus and the liquidus decreases with increasing and decreasing x. On the other hand, data of the Pu–O system are limited and the phase diagram has a lot of uncertainty. Boivineau [35] evaluated the phase diagram of the Pu–O binary system and reported that the solidus and the liquidus of PuO_{2-x} has minimum temperature at O/Pu-ratio of about 1.7. In contrast, Wriedt [36,37] reported that the solidus of nonstoichiometric PuO_{2-x} has a maximum temperature at O/Pu-ratio of about 1.8. In this work the solidus in $(Pu_{0.12}U_{0.88})O_{2-x}$ and $(Pu_{0.2}U_{0.8})O_{2-x}$ increase slightly with decreasing the O/M-ratio as shown in Fig. 7. The variation of the solidus suggests that the phase diagram reported by Wriendt [36,37] is appropriate.

5. Conclusion

The solidus and the liquidus of UO_2 and MOX as a function of the Pu-content and the O/M-ratio were measured by the thermal arrest method. Both temperatures were observed to decrease with increasing the Pu-content and to slightly increase with decreasing the O/M-ratios in the hypo-stoichiometric composition. The solidus of UO_2, $(Pu_{0.12}U_{0.88})O_{2.00}$ and $(Pu_{0.2}U_{0.8})O_{2.00}$ were determined to be 3128 ± 35, 3077 ± 35 and 3052 ± 35 K, respectively. The liquidus of $(Pu_{0.12}U_{0.88})O_{2.00}$ and $(Pu_{0.2}U_{0.8})O_{2.00}$ were determined to be 3117 ± 50 and 3090 ± 50 K, respectively. The solidus and the liquidus of MOX with 29 and 40 at% Pu were also determined, because the data are important for development of nuclear fuels for fast reactors. It was observed that a reaction between MOX and the tungsten capsule occurred during the measurement and phases of metallic tungsten and Pu-oxide were observed in the sample after the measurement. It was concluded that the thermal arrest detected in the measurement of the high Pu-content MOX was not the solidus. Therefore, the solidus and the liquidus of MOX with 29 and 40 at% Pu could not be determined.

Acknowledgements

The authors are pleased to acknowledge Mr. H. Uno, Mr. T. Tamura, Mr. M. Shinada, Mr. S. Shinohara and Mr. M. Kuwana for their collaboration on sample preparation. They also wish to express their thanks to Mr. M. Kowata, Mr. K. Shibata and Mr. H. Sato for their collaboration on ceramography and XRD analyses. Special thanks are also due Dr. T. Mizuno for discussion on the measured data.

References

[1] J.J. Carbajo, G.L. Yoder, S.G. Popv, V.K. Ivanov, J. Nucl. Mater. 299 (2001) 181.
[2] INSC Material Properties Database, Fuel Materials, 12/97.
[3] S.W. Pijanowski, L.S. DeLuca, KAPL-1957, 1960.
[4] T.D. Chikalla, HW-69831, 1961.
[5] T.D. Chikalla, J. Am. Ceram. Soc. 46 (1963) 323.
[6] W.L. Lyon, W.E. Baily, J. Nucl. Mater. 22 (1967) 332.
[7] R.E. Latta, R.E. Fryxell, J. Nucl. Mater. 35 (1970) 195.
[8] E.A. Aitken, S.K. Evans, GEAP-5672, 1968.
[9] K. Konno, T. Hirosawa, J. Nucl. Sci. Technol. 39 (7) (2002) 771.
[10] K. Yamamoto, T. Hirosawa, Y. Yoshikawa, K. Morozumi, S. Nomura, J. Nucl. Mater. 204 (1993) 85.
[11] K. Morimoto, M. Kato, U. Uno, A. Hanari, T. Tamura, H. Sugata, T. Sunaoshi, S. Kono, J. Chem. Solids 66 (2005) 634.
[12] M. Baichi, C. Chatillon, G. Ducros, K. Froment, J. Nucl. Mater. 349 (2006) 57.
[13] M. Koizumi, K. Otsuka, J. Nucl. Sci. Technol. 20 (7) (1983) 529.
[14] R.E. Woodley, J. Nucl. Mater. 96 (1981) 5.
[15] T.M. Besmann, T.B. Lindemer, J. Nucl. Mater. 96 (1981) 5.
[16] M. Kato, T. Tamura, K. Konashi, S. Aono, J. Nucl. Mater. 344 (2005) 235.
[17] R.E. Bedford, G. Bonnier, H. Maas, F. Pavese, Metrologia 33 (1996) 133.
[18] M. Kato, H. Uno, T. Tamura, K. Morimoto, K. Konashi, Y. Kihara, In: Actinides 2005, 4P04, Manchester, July, 2005.
[19] C. Sari, U. Benedict, H. Blank, J. Nucl. Mater. 35 (1970) 267.
[20] G. Kjaerheim, E. Rolstad, Halden Report HPR-107, 1969, p. 36.
[21] T. Tachibana, T. Ohmichi, S. Yamanouchi, T. Itaki, J. Nucl. Sci. Technol. 22 (1985) 155.
[22] J. Komatsu, T. Tachibana, K. Konashi, J. Nucl. Mater. 154 (1988) 38.
[23] C. Ronchi, J.P. Hiernaut, R. Selfslag, G.J. Hylamd, Nucl. Sci. Eng. 113 (1993) 1.
[24] H.J. Matzke, P.G. Lucta, R.A. Verrali, J.P. Hiernaut, Thermophysical properties of UO_2 and SIMFUEL, in: Proceedings of the 22nd International Thermal Conductivity Conference, Tempe, AZ, November 7–10, 1993.
[25] D. Halton, J.P. Hiernaut, M. Sheidlin, C. Ronchi, Advances in laser application for high temperature thermophysical measurements in ceramics, in: Proceedings of the Fourth Euro Ceramics, Karlsruhe, EEC Joint Research Society, 1995.
[26] D. Manara, C. Ronchi, M. Sheindlin, M. Lewis, M. Brykin, Melting of stoichiometric and hyperstoichiometric uranium dioxide, J. Nucl. Mater. 342 (2005) 148.
[27] L.F. Epstein, J. Nucl. Mater. 22 (1967) 340.
[28] M.G. Adamson, E.A. Aitken, R.W. Caputi, J. Nucl. Mater. 130 (1985) 349.
[29] E. Aitken, Letter to K. Uematu, Private Communication, 1976.

[30] T. Fujino, T. Shiratori, N. Sato, K. Fukuda, K. Yamada, H. Serizawa, J. Nucl. Mater. 297 (2001) 176.
[31] S. Yamanaka, J. Sbmiizu, M. Miyake, J. Nucl. Mater. 20 (1993) 27.
[32] J.B. Ainscough, F. Rigby, S.C. Oscorn, J. Nucl. Mater. 52 (1974) 191.
[33] C. Guéneau, M. Baichi, D. Labroche, C. Chatillon, B. Sundman, J. Nucl. Mater. 304 (2002) 161.
[34] P.Y. Chevalier, E. Fisher, B. Cheynet, J. Nucl. Mater. 303 (2002) 1.
[35] J.C. Boivineau, J. Nucl. Mater. 60 (1976) 31–38.
[36] H.A. Wriedt, The O–Pu (oxygen–plutonium) system, Bull. Alloy Phase Diag. 11 (2) (1990) 184.
[37] H.A. Wriedt, T.B. Massalski (Eds.), O–Pu (Oxygen–Plutonium), Binary Alloy Phase Diagrams, ASM International, 1990, p. 2907.